

# Arsenate and Chromate Retention Mechanisms on Goethite. 1. Surface Structure

SCOTT FENDORF,<sup>†</sup> MATTHEW J. EICK,<sup>‡</sup>  
PAUL GROSSL,<sup>\*,§</sup> AND  
DONALD L. SPARKS<sup>‡</sup>

*Soil Science Division, University of Idaho,  
Moscow, Idaho 83844-2339, Department of  
Plant and Soil Sciences, University of Delaware,  
Newark, Delaware 19717-1303, and Department of  
Plant, Soil, and Biometeorology, Utah State University,  
Logan, Utah 84322-4820*

The molecular structure of ions retained on mineral surfaces is needed to accurately model their sorption process and to determine their stability. Extended X-ray absorption fine structure (EXAFS) spectroscopy was used in this study to deduce the local coordination environment of two environmental contaminants, arsenate and chromate, on the mineral goethite ( $\alpha$ -FeOOH). Based on the oxyanion-Fe distances, it was concluded that three different surface complexes exist on goethite for both oxyanions: a monodentate complex, a bidentate-binuclear complex, and a bidentate-mononuclear complex. At low surface coverages, the monodentate complex was favored while at higher coverages the bidentate complexes were more prevalent—the bidentate-binuclear complex appears to be in the greatest proportion at these highest surface coverages. Therefore, modeling efforts for chromate or arsenate retention on goethite need to consider a monodentate complex at very low coverages, both the monodentate and bidentate complexes at intermediate coverages, and predominantly the bidentate complexes at very high coverages.

## Introduction

Arsenic and chromium are potential toxins that enter the environment in elevated levels primarily due to anthropogenic activities. The toxicity of arsenic in biological systems is well established. The mechanism and degree of toxicity depends on its speciation. Arsenate ( $\text{AsO}_4^{3-}$ ) acts as an analog of phosphate ( $\text{PO}_4^{3-}$ ) and can uncouple substrate-level phosphorylation in the glycolytic pathway (1). Arsenite ( $\text{AsO}_3^{3-}$ ) possesses a high affinity for the sulfhydryl groups of amino acids such as cysteine and thereby inactivates a wide range of enzymes in intermediate metabolism (2). As a consequence, arsenite is more toxic than arsenate. Current Federal water quality standards indicate that arsenic concentrations in excess of 50 ppb are hazardous to the welfare of humans and domestic animals (3). Fortunately, arsenate is the

dominant species in oxygenated systems, and like phosphate, generally exhibits a low mobility in soils and waters due to its retention on mineral surfaces. Furthermore, such retention reactions may also help to restrict reduction of As(V) to As(III) under reducing conditions (4), a desirable consequence since As(III) is the more toxic and mobile species.

Chromate is also very toxic to living organisms, being a strong oxidant, a potential carcinogen, and corrosive (5). Chromate is more mobile in soils than arsenate, and its retention mechanism is also unresolved. Modeling efforts of Cr(VI) sorption on hydrous oxides of Fe and Al as well as in soils suggest that Cr(VI) forms an outer-sphere complex on these surfaces (6–9). In contrast to surface complexation modeling, competitive ion displacement studies have shown that Cr(VI) is retained much more strongly than anions such as  $\text{Cl}^-$  or  $\text{SO}_4^{2-}$  and that its retention strength approaches that of phosphate (10, 11). However, these mechanisms are based on macroscopic data that cannot definitively ascertain microscopic information.

Because of the hazards invoked by both arsenate and chromate, reactions that remove these species from the aqueous phase rendering them immobile and limiting their bioavailability are desirable. Hydrous oxides of Fe are one of the principle sorbents of these oxyanions in soils and waters. Knowledge of the oxyanion sorption mechanisms will help in the development of molecular sorption models of such reactions, and it will help to evaluate the risk imposed by the sorbate.

The local coordination environment of arsenate absorbed on and coprecipitated with ferrihydrite was previously investigated using extended X-ray absorption fine structure (EXAFS) spectroscopy (12, 13). The presence of a bidentate-binuclear complex was noted by both Waychunas et al. (12) and Manceau (13) and appears to be the dominant surface complex. The same type of complex was also observed for phosphate (14, 15) and arsenate (16, 17) sorption on goethite using infrared (IR) spectroscopy. In addition to the bidentate-binuclear complex, Waychunas et al. (12) and Manceau (13) noted other surface states of arsenate on ferrihydrite; however, their conclusions are not consistent. Waychunas et al. (12) obtained an optimal fit between predicted and experimental EXAFS curves by including a monodentate surface complex. Manceau (13), on the other hand, proposed a bidentate-mononuclear complex that was similar to the surface structure observed for selenate adsorbed on goethite (18). Recent wide-angle X-ray scattering (WAXS) data lend further support to the bidentate-binuclear complex but showed no indication of a bidentate-mononuclear complex (19); the presence of a monodentate complex could neither be supported or refuted by the WAXS data.

Although the atomic configuration of arsenate on ferrihydrite was investigated previously, further information is needed on the surface structure of arsenate sorbed on other iron oxides common to soils. No direct information on the surface structure of chromate sorbed on hydrous oxides is published. Accordingly, the objective of this study was to determine the surface structure of chromate and arsenate sorbed on a common soil iron oxide, goethite, using EXAFS spectroscopy. This technique is sensitive to the local coordination environment of the oxyanion, yielding direct information on the distances and number of ions about As or Cr. The surface structures derived here are used in the

\* Corresponding author fax: 801-797-3376; e-mail address: grossl@cc.usu.edu.

<sup>†</sup> University of Idaho.

<sup>‡</sup> University of Delaware.

<sup>§</sup> Utah State University.

**TABLE 1. Reaction Conditions for Arsenate and Chromate Sorption on Goethite and Resulting Surface Coverage**

oxyanion	concn (mM)	pH	log $\Gamma^a$	
AsO <sub>4</sub> <sup>3-</sup>	1	9.0	-2.27	
		8.0	-2.15	
		6.0	-2.05	
CrO <sub>4</sub> <sup>2-</sup>	2	6.0	-1.90	
		3	6.0	-1.67
		5	5.0	-1.45

<sup>a</sup> Surface excess based on the quantity of the oxyanion sorbed per mole of Fe in goethite:  $\Gamma = (\text{mol of oxyanion})/(\text{mol of Fe})$ .

second paper of this series (20) to determine the rate of sorption and desorption using a rapid kinetic technique, pressure-jump relaxation.

### Materials and Methods

Reagent-grade Na<sub>2</sub>CrO<sub>4</sub> and Na<sub>3</sub>AsO<sub>4</sub> were reacted individually with a synthetic goethite by batch methods that are described in detail in the following paper (20). A 1 mM AsO<sub>4</sub><sup>3-</sup> solution was reacted with a 10 g/L goethite suspension at various pH values; chromate was reacted at initial concentrations between 1 and 5 mM with the same suspension density. Table 1 provides the surface excess,  $\Gamma_{\text{oxyanion}}$ , based on these reaction conditions. We define the surface excess ( $\Gamma$ ) as the quantity (mol) of sorbate (arsenate or chromate) per mol of Fe in the sorbent (goethite). The surface loadings reported in this study were chosen to reflect the distribution and transition of surface complexes resulting from these ions. The goethite used in this study was synthesized by the methods of Schwertmann and Cornell (21) and had a BET surface area of 50 m<sup>2</sup>/g. The pH was adjusted between values of 4 and 8 using 0.1 M HNO<sub>3</sub> or NaOH and a background electrolyte of 0.1 M NaNO<sub>3</sub>.

After the reagents were dispensed and the pH adjusted to the desired value, the reaction vessels were placed on a reciprocating shaker for 24 h and then filtered through a 0.22- $\mu$ m membrane filter. The effluent was measured for requisite solution As or Cr; the extent of sorption was calculated by the difference between the added concentration of As or Cr and that in solution after the 24-h reaction period. The filtrate was rinsed with distilled, deionized water and sealed in a vial to await EXAFS analysis.

EXAFS spectroscopy was performed on the arsenate- and chromate-reacted goethite solids on beamline X-11A at National Synchrotron Light Source, Brookhaven National Laboratory. The electron storage ring operated at 2.528 GeV with currents ranging from  $\approx$ 215 mA immediately after a fill to a refill current of 110 mA. A sagittally focused beam (22) was used to excite the K-shell of Cr (5989 eV) while the K-shell of As (11867 eV) was probed with an unfocused beam. Higher-order harmonics were rejected by detuning 30% from the maximum incident intensity ( $I_0$ ) for Cr and 20% for As.

The energy range studied for each element was approximately -200 to 1000 eV around their absorption edge. Absorbance of the incident X-rays was measured by the intensity of the resulting fluorescent X-rays using a wide-angle ionization chamber—a Stern—Heald-type detector (23). To help attenuate scattered principle energy X-rays from entering the fluorescent detector, Soller slits and an absorbing filter were placed between the sample and the detector: a V-filter was used for Cr and a Ge-filter for As. Samples were mounted in a 4 × 6 × 25 mm slot cut in an Al block. The sample cell was sealed with 0.0005 in. thick Kapton polyimide film (CHR Industries, type K-104) to prevent moisture loss while minimizing X-ray absorption. The reported spectra were obtained at 77 K to reduce the thermal disorder of the specimen. Further details on the XAFS procedure can be found elsewhere (24).

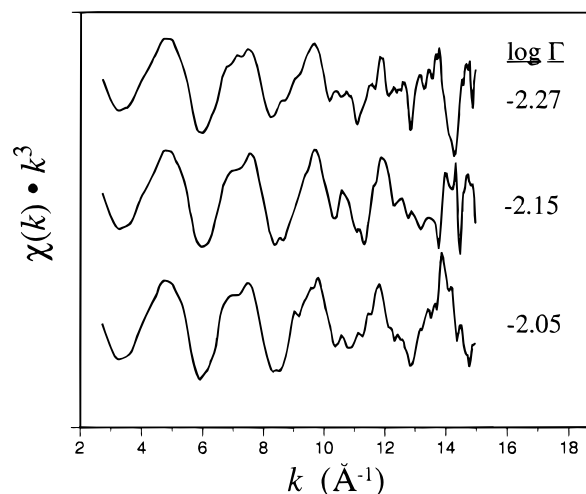


**FIGURE 1. Experimental EXAFS spectra, weighted by  $k^3$ , of arsenate sorbed on goethite at surface loadings ( $\log \Gamma_{\text{as}}$ , mol/mol) of -2.27, -2.18, and -2.07.**

At least three collected fluorescence spectra were averaged, the background absorbance of the spectra was removed, and the atomic absorption was normalized to unity. To isolate the scattering contribution of the spectra, which result from the coordination environment of the absorber, a spline function was fit to the 'absorption envelope' and subtracted from the spectra; the spline function was used to account for the atomic absorption in the absence of a coordinating field. The isolated structural function was then transformed from units of eV to  $\text{\AA}^{-1}$ . This results in a curve comprised of the scattering contributions of the spectra. The  $\chi(k)$  function was Fourier transformed (FT) in order to isolate the contribution of different coordinating shells. Each major peak below 4  $\text{\AA}$  in the FT curve was isolated and backtransformed; selection of the window was based on the minimum amplitude points at low and high distance points around a peak. Additionally, the full FT (ca. 1–3.5  $\text{\AA}$ ) was backtransformed for final fitting. This gives a Fourier filtered  $\chi(k)$  function of the peak constituents. The Fourier filtered spectra were then fit with the predicted function in which the number of coordinating atoms (CN), their distance ( $R$ ), and disorder ( $\sigma^2$ ) were varied to give the best fit between the experimental and predicted spectra. Values of the energy shift were based on optimal fits of the first shell (As-O or Cr-O) and were subsequently fixed at these values for higher shell fitting. Phase and amplitude functions for the absorber and backscatters were defined using the FEFF model (25–27). After each of the individual peaks in the FT spectra were backtransformed and fit, the entire spectra was modeled using the same parameters. This procedure resulted in first shell accuracy of  $N = \pm 20\%$  and  $R = \pm 0.02 \text{\AA}$ ; the accuracy decreases for more distant shells.

### Results

EXAFS spectroscopy was employed to determine the local coordination environment of Cr(VI) and As(V) sorbed on goethite. The experimental  $\chi(k)$  spectra of As(V) sorbed on goethite at three different initial loadings are shown in Figure 1. Fourier transformation of the  $\chi(k)$  function leads to a radial structure function (RSF), in which the peak positions correspond to the interatomic distances within the material (Figure 2). These peak positions, however, are uncorrected for phase shifts so that the positions are slightly shifted from the true interatomic distances. By backtransforming the spectra, a theoretical model can be fit to the experimental spectra yielding  $R$ , CN, and  $\sigma^2$  based on the optimized fit. After the parameters of each peak were determined, the full Fourier filtered  $\chi(k)$  function from 0 to 4  $\text{\AA}$  was fit to substantiate the local coordination environment.

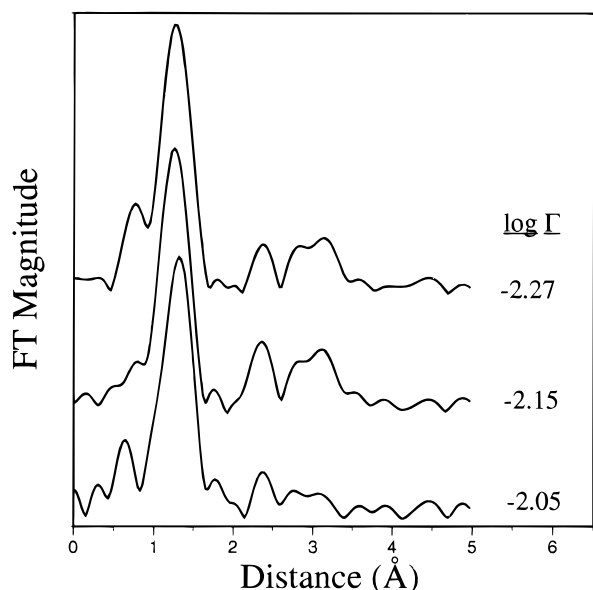


FIGURE 2. Fourier-transformed spectra of As(V) resulting in a radial structure function. The peak positions correspond to the distances of the atomic shells but are uncorrected for phase shifts.

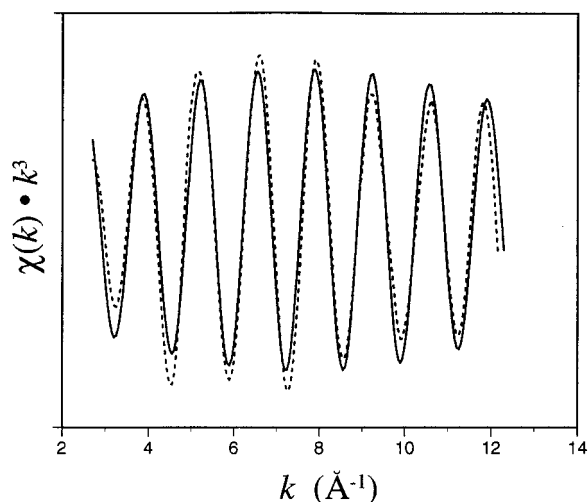


FIGURE 3.  $k^3$  weighted, backtransformed higher distant peaks from the FT spectra of As on goethite showing the fit (dashed line) of the theoretical curve to the experimental curve (solid line).

Based on the fit of the theoretical to the experimental spectra, the first peak in the FT curve was composed of approximately four oxygen atoms at an average distance of 1.66 Å from the central As atom. Peaks occurring at greater distances in the FT spectra were also isolated and fit. The more distant peaks resulted from backscattering induced by Fe atoms, and the CN and  $R$  values varied with the different surface loadings. At the highest loading, a shell at 3.24 Å dominated the backtransformed curve, with the fits being significantly improved by the addition of shells at 2.85 and 3.59 Å. The highest distant Fe backscatter was much more prominent at the lowest surface loading. The fit of a backtransformed second peak is shown in Figure 3. After each of the peaks in the FT spectra were fit, the parameters were used to model the backtransformed curve composed of the full spectra out to approximately 4 Å. The fits of the full spectra for each arsenate loading are shown in Figure 4. The local coordination parameters determined by this procedure for As are summarized in Table 2.

In Figure 5, the experimental EXAFS spectra for Cr(VI) sorbed on goethite are shown for three different surface loadings. Chromate exhibited a similar first shell environment

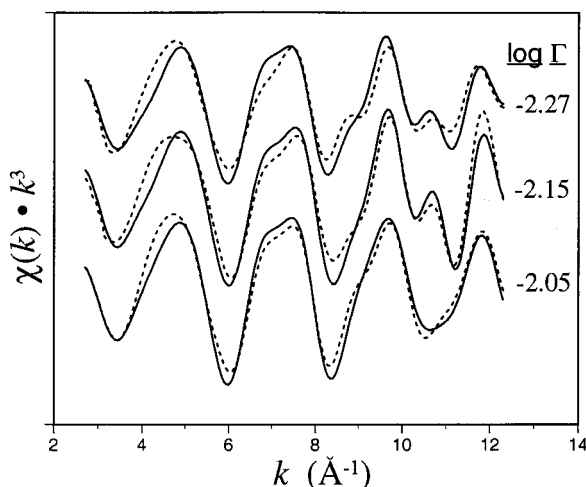


FIGURE 4. Full shell,  $k^3$  weighted backtransformed spectra (0 to  $\approx$  4 Å in the FT spectra) of arsenate on goethite illustrating the best fit (dashed line) obtained for the experimental spectra (solid line).

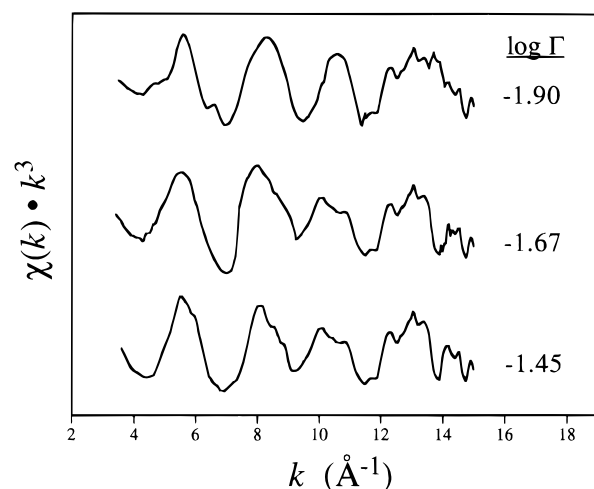


FIGURE 5. Experimental EXAFS spectra, weighted by  $k^3$ , of chromate sorbed on goethite at surface loadings ( $\log \Gamma_{Cr}$ , mol/mol) of -1.90, -1.67, and -1.45.

TABLE 2. Parameters Defining Local Coordination Environment of Arsenate Sorbed on Goethite as Determined by EXAFS Spectroscopy

surface excess, $\log \Gamma$	shell	distance (Å)	CN	$\sigma^2$ (Å <sup>2</sup> )
-2.05	As-O	1.66	3.8	0.0018
	As-Fe	2.85	1.3	0.0022
		3.24	1.6	0.0031
		3.59	0.41	0.0055
-2.15	As-O	1.66	3.7	0.0019
	As-Fe	2.84	0.92	0.0026
		3.23	1.3	0.0029
		3.59	0.67	0.0062
-2.27	As-O	1.67	3.9	0.0019
	As-Fe	2.85	0.61	0.0017
		3.24	0.96	0.0038
		3.60	1.05	0.0050

to that of arsenate: for all three surface coverages approximately four oxygen atoms coordinate the central Cr atom at an average distance of 1.68 Å. This distance and coordination number are in agreement with values reported for the chromate ion (28). Beyond the first shell composed of oxygen, multiple Fe shells are apparent. Fitted backtransformed spectra of the isolated peaks in the FT spectra and the full backtransformed spectra from 0 to 4 Å (Figure 6)

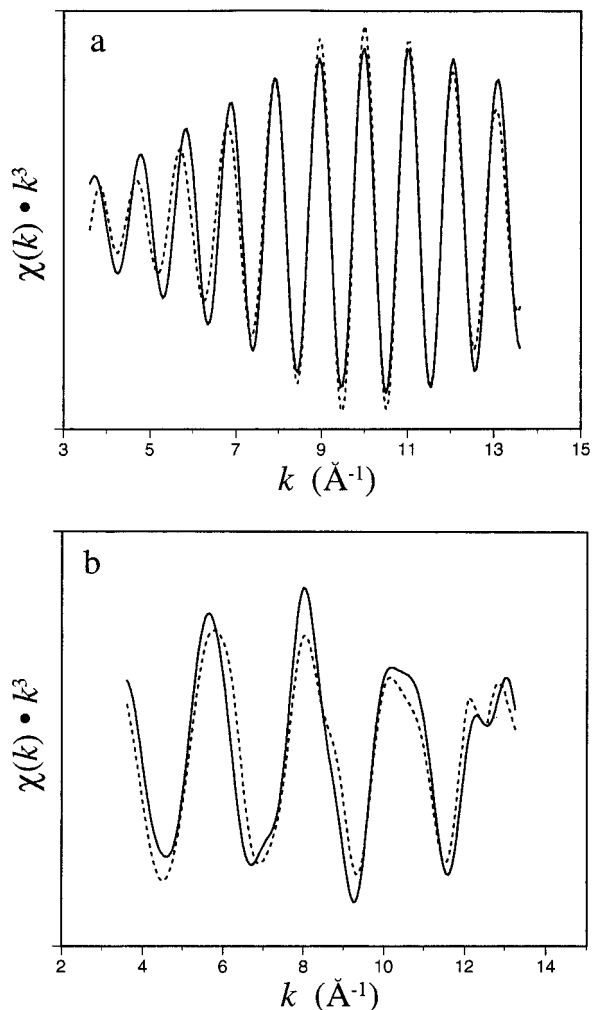


FIGURE 6. Theoretical fits (dashed lines) of the  $k^3$  weighted isolated higher distant peaks (a) and full spectra from 0 to 4 Å (b) of chromate sorbed on goethite at  $\log \Gamma = -1.45$ .

TABLE 3. Parameters Defining Local Coordination Environment of Chromate Sorbed on Goethite as Determined by EXAFS Spectroscopy

surface excess, $\log \Gamma$	shell	distance	CN	$\sigma^2$ (Å <sup>2</sup> )
-1.45	Cr-O	1.69	3.9	0.0025
	Cr-Fe	2.91	0.91	0.0014
		3.29	1.4	0.0025
-1.67	Cr-O	1.68	3.9	0.0019
	Cr-Fe	2.91	0.42	0.0011
		3.27	1.5	0.0021
-1.90	Cr-O	1.68	3.9	0.0019
	Cr-Fe	3.29	1.0	0.0020
		3.63	0.8	0.0031

indicate that Fe atoms reside dominantly at distances of 3.29 Å; an additional distance of 3.63 Å was necessary to describe the lowest surface loading ( $\log \Gamma = -1.90$ ). Additionally, the fits of the higher two coverages ( $\log \Gamma = -1.45$  and  $-1.67$ ) were improved with the addition of an Fe shell at 2.91 Å. The parameters defining the local coordination environment of Cr(VI) on goethite are summarized in Table 3.

## Discussion

The oxyanions of As(V) and Cr(VI) sorbed on goethite exhibit somewhat similar local environments. Three different oxyanion-Fe distances were observed for all surface coverages

of arsenate on goethite, while two distances, which changed with surface coverage, were observed for chromate. The most distant shells, 3.59 Å for As-Fe and 3.63 Å for Cr-Fe, are characteristic of linear arrangements, corner sharing tetrahedra-octahedra, resulting from a monodentate surface complex. The monodentate complex was more pronounced at low arsenate surface coverages and was only apparent in the EXAFS spectra the lowest surface coverages investigated for chromate. The most prominent distances observed for all surface coverages of each oxyanion, 3.24 Å for As-Fe and 3.29 Å for Fe-Cr, are intermediate between the edge and corner-sharing distances; they represent a bidentate-binuclear complex in which the corner-sharing octahedra-tetrahedra do not result in a linear arrangement. At the higher surface coverages for both As and Cr, an improved prediction of the EXAFS spectra was obtained by including a third Fe-oxyanion distance. These shortest As-Fe (2.85 Å) and As-Cr (2.91 Å) distances result from an edge sharing of the oxyanion tetrahedra and the Fe octahedra; thus, these distances are indicative of a bidentate-mononuclear complex. The surface complexes of chromate and arsenate on goethite are shown schematically in Figure 7 based on the description obtained by EXAFS spectroscopy.

It is apparent from the EXAFS results summarized in Tables 2 and 3 that the surface complexes of Cr(VI) and As(V) change with surface coverage. At lower surface coverages, the monodentate complex is more prominent than at high coverages; with increasing coverage the spectra have an increasing contribution from the bidentate surface complexes. In addition, while the coordination numbers are somewhat qualitative (at best accurate to within 20%), their values for both bidentate complexes, particularly the bidentate-binuclear complex, increase with surface coverage. Therefore, it appears that the monodentate complex represents a significant portion of surface-complexed oxyanions at low surface coverage with diminishing proportions relative to the bidentate complexes at higher surface coverage.

While the EXAFS spectra at the highest loadings of chromate are dominated by the bidentate complexes, it should be noted that monodentate complexes may be present, and almost certainly are, at the higher coverages. Their contribution, however, is masked by the dominance of the bidentate complexes signal in the EXAFS spectra, which represents the 'average' local environment. The greater contribution of the bidentate complex occurs due to a predominance of this complex and from the greater backscattering intensity of these closer shells. Since the monodentate complex results in a greater Cr-Fe distance, its contribution to the EXAFS spectra will be diminished relative to the shorter Cr-Fe distances of the bidentate complexes. That is, even when equal proportions of a monodentate and bidentate complex are present, the EXAFS spectra would have a greater contribution from the bidentate complex simply due to the shorter As-Fe distances. Furthermore, for the bidentate-binuclear complex two Fe atoms will contribute to the backscattering for each complexed As species, thus enhancing its influence on the resulting spectra. Nevertheless, comparison of the parameters derived by EXAFS spectroscopy at the different surface coverages does provide important information on the significant surface complexes.

A linear, monodentate arrangement of arsenate must form on a goethite surface functional group that is singly coordinated to a central Fe atom. The formation of a monodentate complex at very low coverage is in agreement with the expected reactivity of the goethite surface based on the description of Hiemstra et al. (29) and on the surface group reactivity proposed by McBride (30). It is also consistent with infrared spectroscopic data that indicate singly coordinated O(H) groups being most reactive with arsenate (17) and phosphate (14, 15). With continued increases in surface coverage, oxyanion complexation to neighboring singly

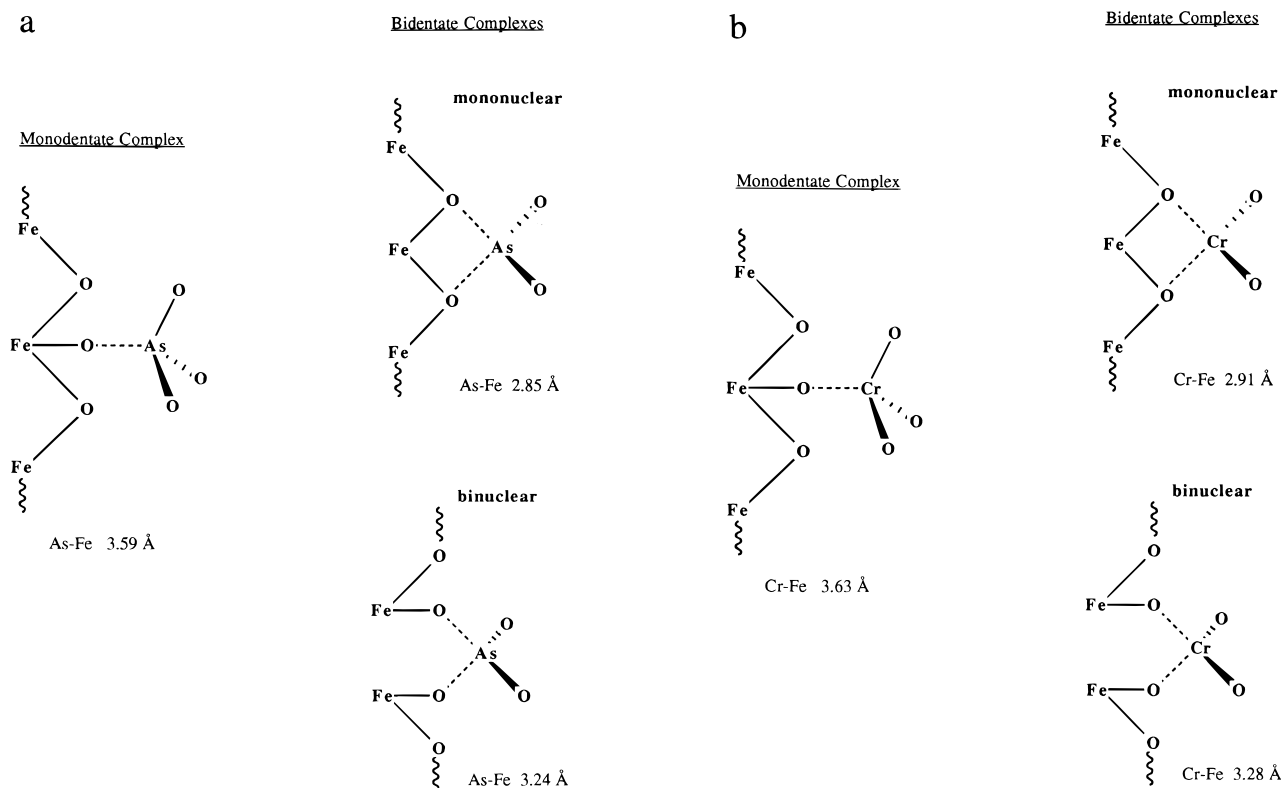


FIGURE 7. Schematic illustration of the surface structure of As(V) and Cr(VI) on goethite based on the local coordination environment determined with EXAFS spectroscopy.

coordinate surface functional groups leads to the formation of a binuclear-bidentate surface complex. The bidentate-binuclear complex appears to be the most prevalent at all but very low surface coverage. This observation is in agreement with WAXS (19), IR spectroscopy (17), and other EXAFS spectroscopy (12, 13) studies. A recent IR study (17) indicates that only singly coordinated surface groups of goethite are reactive with arsenate at coverages below  $\log \Gamma = -1.75$  (200 mmol/kg). Moreover, a bidentate-binuclear complex of arsenate on the (110) face of goethite was predicted as the dominant surface species based on the surface coverage that results in complete disappearance of the singly coordinated surface group vibration mode (17). Similar results were reported for phosphate sorption on goethite (14, 15, 31).

Finally, a bidentate-mononuclear surface complex was also observed at the higher surface coverages investigated. A larger distortion of the goethite surface groups must occur in this configuration (19), and thus a larger activation energy may limit the formation of this complex to conditions conducive to high surface coverage. This type of complex, but in a much higher proportion, was also observed for selenate adsorption on goethite (18). Thus, although the reactivity of specific surface groups on goethite are not fully substantiated, the resulting surface complex discerned by EXAFS spectroscopy presented here agree with the expected reactivity based on current predictions (19, 29, 30) and other spectroscopic studies (12, 13, 17, 19).

In the preceding discussion, we primarily refer to the structural environment of As or Cr resulting from changes in surface coverage. However, one must also consider the fact that the pH for many of these systems was also changed. This is particularly true for As in which the pH was changed for each of the different loadings. Thus, it is possible that the different surface structures are also a consequence of oxyanion protonation.

Knowledge of surface structures is needed for accurate mechanistic models of arsenate and chromate retention on minerals in soils and sediments. Moreover, the stability of

the sorbate will be dependent upon its molecular configuration. EXAFS spectroscopy indicates that three surface complexes of both arsenate and chromate exist on goethite. At very low surface loadings, a monodentate complex must be considered. At high surface coverages, the sorption of these oxyanions is dominated by the formation of bidentate surface complexes. It appears that the bidentate-binuclear complexes are the most significant at all but very low surface coverage.

## Literature Cited

- (1) Stryer, L. *Biochemistry*; W. H. Freeman: New York, 1981.
- (2) Ehrlich, H. L. *Geomicrobiology*; Marcel Dekker: New York, 1990.
- (3) *Code of Federal Regulations*. U.S. Government Printing Office: Washington, DC, 1990; p 559.
- (4) McGeehan, S. L.; Naylor, D. V. *Soil Sci. Soc. Am. J.* **1993**, *58*, 337–342.
- (5) National Research Council. *Chromium*; National Academy of Science Publishing: Washington, DC, 1974.
- (6) Ainsworth, C. C.; Girvin, D. C.; Zachara, J. M.; Smith, S. C. *Soil Sci. Soc. Am. J.* **1989**, *53*, 411–418.
- (7) Benjamin, M. M.; Bloom, N. S. In *Adsorption from aqueous solution*; Tewari, P. H., Ed.; Plenum Press: New York, 1981; pp 41–61.
- (8) Zachara, J. M.; Ainsworth, C. C.; Cowan, C. E.; Resch, C. T. *Soil Sci. Soc. Am. J.* **1989**, *53*, 418–428.
- (9) Zachara, J. M.; Girvin, D. C.; Schmidt, R. L.; Resch, C. T. *Environ. Sci. Technol.* **1987**, *21*, 589–594.
- (10) Bartlett, R. J.; Kimble, J. M. *J. Environ. Qual.* **1976**, *5*, 383–386.
- (11) Griffin, R. A.; Au, A. K.; Frost, R. R. *Environ. Sci. Health* **1977**, *A12* (8), 431–449.
- (12) Waychunas, G. A.; Rea, B. A.; Fuller, C. C.; Davis, J. A. *Geochim. Cosmochim. Acta* **1993**, *57*, 2251–2270.
- (13) Manceau, A. *Geochim. Cosmochim. Acta* **1995**, *59*, 3647–3653.
- (14) Atkinson, R. J.; Parfitt, R. L.; Smart, R. St. C. *J. Chem. Soc. Faraday Trans. 1* **1974**, *70*, 1472–1479.
- (15) Parfitt, R. L.; Russell, J. D.; Farmer, V. C. *J. Chem. Soc. Faraday Trans. 1* **1976**, *72*, 1082–1087.
- (16) Lumsdon, D. G.; Fraser, A. R.; Russell, J. D.; Livesey, N. T. *J. Soil Sci.* **1984**, *35*, 381–386.
- (17) Sun, X.; Doner, H. *J. Soil Sci.* In press.

- (18) Manceau, A.; Charlet, L. *J. Colloid Interface Sci.* **1994**, *168*, 87–93.
- (19) Waychunas, G. A.; Fuller, C. C.; Rea, B. A.; Davis, J. A. *Geochim. Cosmochim. Acta* **1996**, *60*, 1765–1781.
- (20) Grossl, P. R.; Eick, M. J.; Sparks, D. L.; Goldberg, S.; Ainsworth, C. C. *Environ. Sci. Technol.* **1997**, *31*, 321–326.
- (21) Schwertmann, U.; Cornell, R. M. *Iron oxides in the Laboratory. Preparation and characterization*; VCH Publishers: New York, 1991.
- (22) Lamble, G. M.; Heald, S. M. *Rev. Sci. Instrum.* **1991**, *63*, 880–884.
- (23) Stern, E. A.; Heald, S. M. *Rev. Sci. Instrum.* **1979**, *50* (12), 1579–1582.
- (24) Fendorf, S. E.; Stapleton, M. G.; Lamble, G. M.; Kelley, M. J.; Sparks, D. L. *Environ. Sci. Technol.* **1994**, *28*, 284–289.
- (25) Mustre de Leon, J.; Rehr, J. J.; Zabinsky, S. I.; Albers, R. C. *Phys. Rev. B* **1991**, *44*, 4146.
- (26) Rehr, J. J.; Albers, R. C.; Mustre de Leon, J. *Phys. B* **1989**, *158*, 417.
- (27) Rehr, J. J.; Mustre de Leon, J.; Zabinsky, S. I.; Albers, R. C. *J. Am. Chem. Soc.* **1991**, *113*, 5135.
- (28) Wells, A. F. *Structural Inorganic Chemistry*; Oxford University Press: New York, 1984.
- (29) Hiemstra, T.; DeWit, J. C. M.; Van Riemsdijk, W. H. *J. Colloid Interface Sci.* **1989**, *133*, 91–104.
- (30) McBride, M. B. *Environmental Chemistry of Soils*; Oxford University Press: New York, 1994.
- (31) Torrent, J.; Barron, V.; Schwertmann, U. *Soil Sci. Soc. Am. J.* **1990**, *54*, 1007–1012.

Received for review September 6, 1995. Revised manuscript received September 11, 1996. Accepted September 11, 1996.<sup>⊗</sup>

ES950653T

<sup>⊗</sup> Abstract published in *Advance ACS Abstracts*, November 15, 1996.